International Journal of Adhesion and Adhesives 85 (2018) 149–156

Contents lists available at ScienceDirect

International Journal of Adhesion and Adhesives

journal homepage: www.elsevier.com/locate/ijadhadh

Fatigue crack propagation rate of CFRP/aluminum adhesively bonded DCB joints with acrylic and epoxy adhesives

Makoto Imanaka[a,*], Kiyoshi Ishii[b], Keisuke Hara[c], Toru Ikeda[d], Yosuke Kouno[e]

[a] Department of Technology Education, Osaka University of Education, Kashiwara, Osaka 582-8582, Japan
[b] Faculty of Junior College of Automobile Industry, Osaka Sangyo University, Nakagaito Daito City, Osaka 574-8530, Japan
[c] National Institute of Technology, Yonago College, Hokona Yonago, Tottori 683-8502, Japan
[d] Department of Mechanical Engineering, Kagoshima University, Korimoto Kagoshima, Kagoshima 890-0065, Japan
[e] Western Region Industrial Research Center, Hiroshima Prefectural Technology Research Institute, Agaminai Kure City, Hiroshima 737-0004, Japan

ARTICLE INFO

Keywords:
Fatigue crack propagation rate
Double cantilever-beam specimen
Carbon-fiber-reinforced plastics
Adhesively bonded joint
Residual stress

ABSTRACT

Recently, structural acrylic adhesives have received increased interest because they can be cured at room temperature. However, there are few studies investigating the strength behavior of CFRP/metal joints bonded with acrylic adhesive, especially under cyclic loading. In this study, the fatigue crack growth rate was measured using adhesively bonded CFRP/aluminum double cantilever beam (DCB) joints made with an acrylic adhesive. To compare fatigue crack growth behavior with heat-cured type adhesive, fatigue testing was also conducted for DCB joints with an epoxy adhesive. For CFRP/aluminum asymmetrical joints, the ratio of the thickness of the lower adherend to the upper adherend is an important factor determining the mode ratio and stress distribution at the crack tip which are affected by the residual stress generated in the curing process. The effect of the thickness ratio for the DCB joints on the fatigue crack growth rate was investigated for DCB joints with both acrylic and epoxy adhesives.

1. Introduction

Fiber reinforced composites plastics (CFRP) are widely used in various engineering industries such as aerospace, automobile, marine, because of their significant advantage in terms of strength-to-weight and stiffness-to-weight ratios. These materials demand composite bonded joints as a structural element. Adhesive joints have several advantages from the viewpoint of joint strength when compared with other bolted joints or riveted joints. Hence, it is important to clarify the strength characteristics of these joints, particularly under cyclic loading, because many CFRP structures are subjected to cyclic load due to vibration and power transmission. Hence, there are many studies about fatigue behavior for CFRP/CFRP bonded joints [1–8]. However, it is rare to create structures having only CFRP components; CFRP-to-metal bonding is necessary. However, in the present situation there have been fewer studies on the fatigue behavior of CFRP/metal bonded joints [9–13].

Incidentally, fatigue life is the sum of initiation life and propagation life. The former fatigue initiation life is defined the number of cycles before the macro-crack forms. For example adhesively bonded lap joints, the initiation life relates to the stress field in the vicinity of the lap end, wherein a stress singularity parameter was used as a fatigue initiation criterion [14,15]. Experimentally, back-face strain measurement method has been used to monitor the fatigue crack initiation for the lap joints [16]. The latter propagation life is the number of cycles from macro crack initiation to unstable fracture, which is usually calculated based on the fatigue crack growth rate that is a function of stress intensity factor or energy release rate [15]. In the present study, only the fatigue crack propagation behavior is treated.

The fatigue crack propagation behavior of CFRP/metal bonded joints is very complex, because the CFRP/metal bonded joint consists of substrates having extremely different material constants. For example, CFRP/metal bonded DCB joints always have a mode II component at the crack tip even under tensile loading due to an asymmetrical combination of the adherends. Since the fatigue crack propagation behavior is affected by the mode-mixity at the crack tip, the mixed-mode failure criterion is necessary for evaluate the fatigue crack propagation rate of the CFRP/metal bonded joints. Several mixed-mode criterion have been proposed [10,15,17]. The most common mixed failure criterion is the total strain energy release rate, $G_T = G_I + G_{II}$ [15,17]. Hence, in this study the total energy release rate was used to evaluate the crack growth rate.

In the present situation, structural epoxy adhesives are normally used to bond these substrates, and most structural epoxy adhesives

* Corresponding author.
E-mail address: imanaka@cc.osaka-kyoiku.ac.jp (M. Imanaka).

https://doi.org/10.1016/j.ijadhadh.2018.06.003
Accepted 1 June 2018

require a heat curing process. Hence, residual stress appears in the adhesive layer during the curing cycle of the adhesive due to the difference in thermal expansion coefficient between the CFRP and metallic substrates. The residual stress thus generated affects the joint strength.

To reduce the effect of the residual stress, it is desirable to cure adhesively bonded joints at room temperature. Recently, structural acrylic adhesives have been of special interest because the acrylic adhesives can be cured at room temperature within a relatively short time and require less surface preparation. However, studies investigating the strength behavior of the joints bonded with acrylic adhesives are few compared to those concerning epoxy adhesives [18–24].

In this study fatigue crack growth behavior was investigated using adhesively bonded CFRP/aluminum double cantilever beam (DCB) joints made with an acrylic adhesive. To compare the fatigue crack growth behavior with heat-cured type adhesive, fatigue tests were also conducted for DCB joints made with an epoxy adhesive. For CFRP/aluminum asymmetrical DCB joints, the thickness ratio of the CFRP adherend to the metallic one is an important factor determining the mode ratio, G_{II}/G_I at the crack tip. Moreover, the residual stress generated in the curing process affects the mode ratio. The fatigue crack growth behavior of DCB joints with the acrylic adhesive was compared with that with the epoxy adhesive, wherein the thickness ratio of the CFRP adherend to the metallic one was varied. Furthermore, the mode ratio, G_{II}/G_I at the crack tip and crack propagation path were simulated by the finite element method.

2. Experimental procedure

2.1. Materials and adhesively bonded specimens

Fig. 1 shows the shapes and sizes of the adhesively bonded DCB specimens used for the fatigue tests. The adherends used were aluminum alloy (JIS 2017-T4) and a unidirectional CFRP composite whose carbon fiber and matrix epoxy resin were Mitsubishi Rayon, TR505 and #350, respectively. Two kinds of adhesive were used; an acrylic adhesive (NS-770M25, Denka Co. Ltd.), and a one-part epoxy adhesive (E56S, Sunrise MSI Co. Ltd.). To investigate the effect of aluminum adherend thickness on fatigue crack propagation behavior, three types of joint with different thicknesses of aluminum adherend were fabricated, wherein flexural stiffness ratios of aluminum adherends (t = 3 mm,5 mm,10 mm) to CFRP adherend (t = 3 mm) are 0.55, 2.54 and 20.39.

The adhesively-bonded DCB joints were prepared as follows: The bonding surface of the CFRP adherends was polished with grade 120 emery paper under dry conditions, and that of the aluminum adherends was phosphoric-acid anodized followed by application of an epoxy primer. As in Fig. 1, a filler gauge of 0.01-mm thickness treated with a release agent was used as a pre-crack between Teflon tapes. The DCB joints bonded with the epoxy adhesive were cured at 160 °C for 1 h, and the joints bonded with acrylic adhesive were cured at room temperature for 24 h. The resulting joint specimens were supplied for fatigue tests.

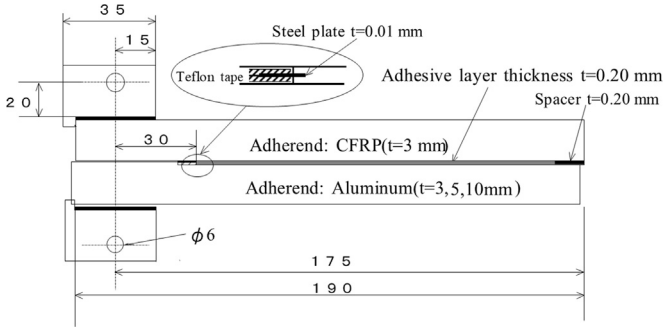

Fig. 1. Shape and dimensions of the adhesively bonded DCB joints.

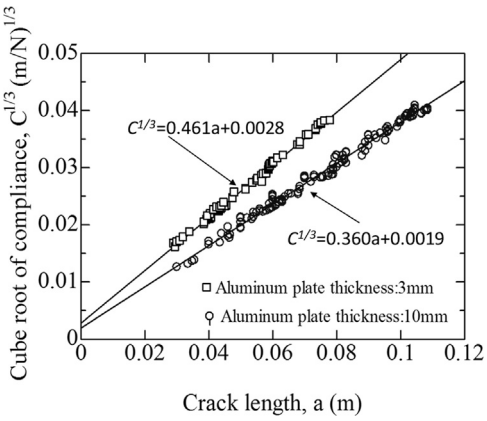

Fig. 2. Relationship between crack length and cube root of compliance, $C^{1/3}$.wherein CFRP plate thickness is 3 mm.

2.2. Fatigue test procedure

Fatigue tests were carried out under displacement control, where the waveform was sinusoidal with a loading frequency f = 2 Hz and a displacement ratio R ($\delta_{min}/\delta_{max}$) = 0.2. The fatigue crack growth measurement were conducted after slightly advancing fatigue crack from the tip of initially induced steel plate as in Fig. 1. In the displacement control, the strain energy release rate, G continuously decreases with increasing crack length until the crack growth is finally arrested.

For adhesively bonded symmetrical and asymmetrical DCB specimens, there is a known linear relationship between the crack length, a, and the cube root of compliance, $C^{1/3}$, as shown in Eq. (1),

$$C^{1/3} = pa + q \tag{1}$$

Where p and q are regression coefficients. Fig. 2 shows the relationship between the cube root of compliance and crack length for the two types of CFRP/aluminum DCB joints, where the compliance was obtained from the relationship between the displacement between the loading points, δ and applied load, P during the unloading portion.

As shown in this figure, the linear relationship between the cube root of compliance and crack length is observed for both the CFRP/aluminum joints, irrespective of the thickness of the aluminum plates. In this fatigue test, the crack length was occasionally measured using a traveling microscope, and it agreed with the calculations using Eq. (1). Thus, the crack length, a, was determined by the compliance method.

The strain energy release rate is calculated by the following equation:

$$G = \frac{P^2}{2}\frac{dC}{da} \tag{2}$$

Where P is applied load, B is the width of the specimen, a is crack length and C is compliance. dC/da, was calculated from Eq. (1).

3. Finite element analysis

Generally, the mode ratio, G_{II}/G_I at the crack tip governs the crack propagation behavior. For adhesively bonded CFRP/aluminum DCB joints, the mode ratio, G_{II}/G_I at the crack tip varies with the thickness ratio of the CFRP to the aluminum adherends due to asymmetrical combination of the adherends. Moreover, the difference in thermal expansion coefficient between CFRP and aluminum causes residual thermal stress during cooling from the curing temperature for an epoxy adhesive, which also affects the mode ratio and crack propagation behavior. To investigate the effect of the thickness ratios of the adherend on the mode ratio and crack propagation path, finite element analysis was carried out for the CFRP/aluminum DCB joints with the acrylic and

epoxy adhesives, wherein the finite element code was MSC-Marc, and quadrangle and triangle plane strain elements were used.

Although the elastic range of the acrylic adhesive is small, the load range in the fatigue test is also small. So, we deal with it as an elastic body for the sake of convenience. In this analysis, the energy release rates of the DCB joints under mode I and II loading conditions were calculated using the VCCT in the MSC-Marc program under the assumption that the adhesives and adherends were elastic materials. We would like to analyze the acrylic adhesive taking nonlinearity into consideration in future.

When the crack propagates at the adherend /adhesive layer interface, the stress oscillates in the vicinity at the crack tip, wherein a complicated problem arises that the mode ratio depends on the distance from the crack tip [25]. Fortunately, in this experiment cracks propagated inside the adhesive layer or CFRP, so we did not consider the problem of interfacial crack.

The mode ratios were then calculated using the obtained energy release rates. In mixed mode condition, crack initiation was conducted individual mode criterion. When the energy release rate of the elements around the existing crack tip is fulfilled as $G_I > G_{Ic}$ or $G_{II} > G_{IIc}$, then the crack propagates. Since mode I is dominant in this asymmetry DCB specimens, we have considered only Mode I component in crack propagation. The crack initiation simulation was conducted under the assumption that the crack proceeds when the element around the existing crack tip satisfies this failure criterion ($G_I > G_{Ic}$).

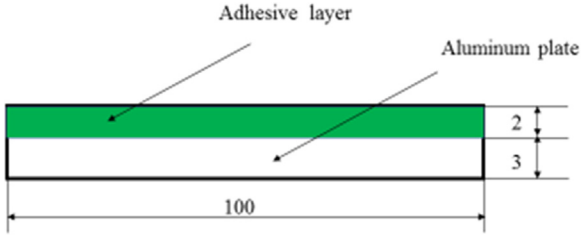

Fig. 4. Adhesive/aluminum plate specimen (width 10 mm).

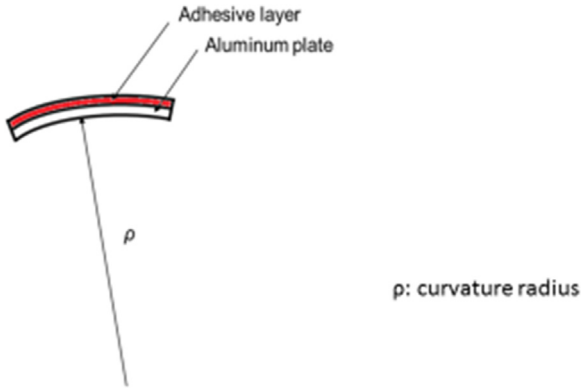

Fig. 5. Schematic illustration of the adhesive/aluminum plate specimen during the cooling process from the curing temperature.

3.1. Measurement of material constants required in the FEM analysis

Two kinds of experiment were conducted to measure the material constants required in the FEM analysis. Elastic constants of the adhesives were obtained from the stress-strain curves using bulk dumbbell specimens as Fig. 3.

The epoxy adhesive used in this experiment requires a heat curing process. Hence, residual stress appears in the adhesive layer during cooling process from the curing temperature to room temperature due to shrinkage of the epoxy adhesive. To evaluate this residual stress, the following experiment was conducted. At first, an adhesive/aluminum plate specimen consisting of the epoxy adhesive and aluminum plate as in Fig. 4 was prepared, wherein the adhesive was pasted on the aluminum plate, then cured in a furnace. During the cooling process, the specimen bent due to the residual stress in the adhesive layer as in Fig. 5.

This specimen was then placed in a furnace. The temperature in the furnace was increased stepwise, while the temperature in the furnace was kept constant the z directional displacement distribution of the specimen was measured by scanning the distance from a laser displacement meter to the specimen, wherein the resolution of the displacement meter is 0.2 μm. An example of z directional displacement is shown in Fig. 6(a). Based on the displacement distribution, the radius of the specimen, ρ was evaluated at each temperature. Fig. 6(b) shows the relationship between $1/\rho$ and temperature for the adhesive/aluminum plate specimen. As shown in this figure, $1/\rho$ decreased with increasing temperature until 80 °C. Above this temperature $1/\rho$ had a nearly constant value. This means that the residual stress in the adhesive layer can be neglected above 80 °C which corresponds to the stress-free temperature. That is, the residual stress appears during cooling from 80 °C to 25 °C (room temperature). Under the assumption that the specimen bends due to the mismatch of thermal expansion coefficient between the adhesive and aluminum plates, the apparent thermal expansion coefficient of the adhesive was evaluated based on the temperature change, ΔT = 80–25° C, using the curvature radius of the adhesive/aluminum plate specimen at room temperature. The

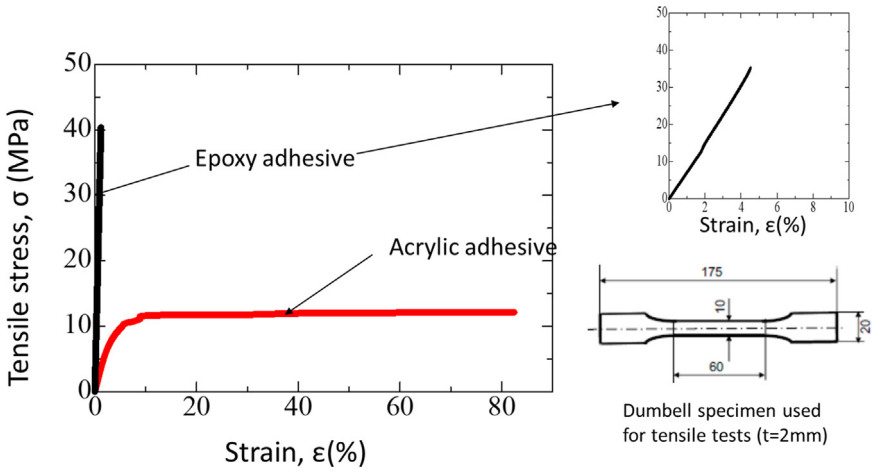

Fig. 3. Stress-strain curve of the adhesives, wherein the measurements were conducted under room temperature.

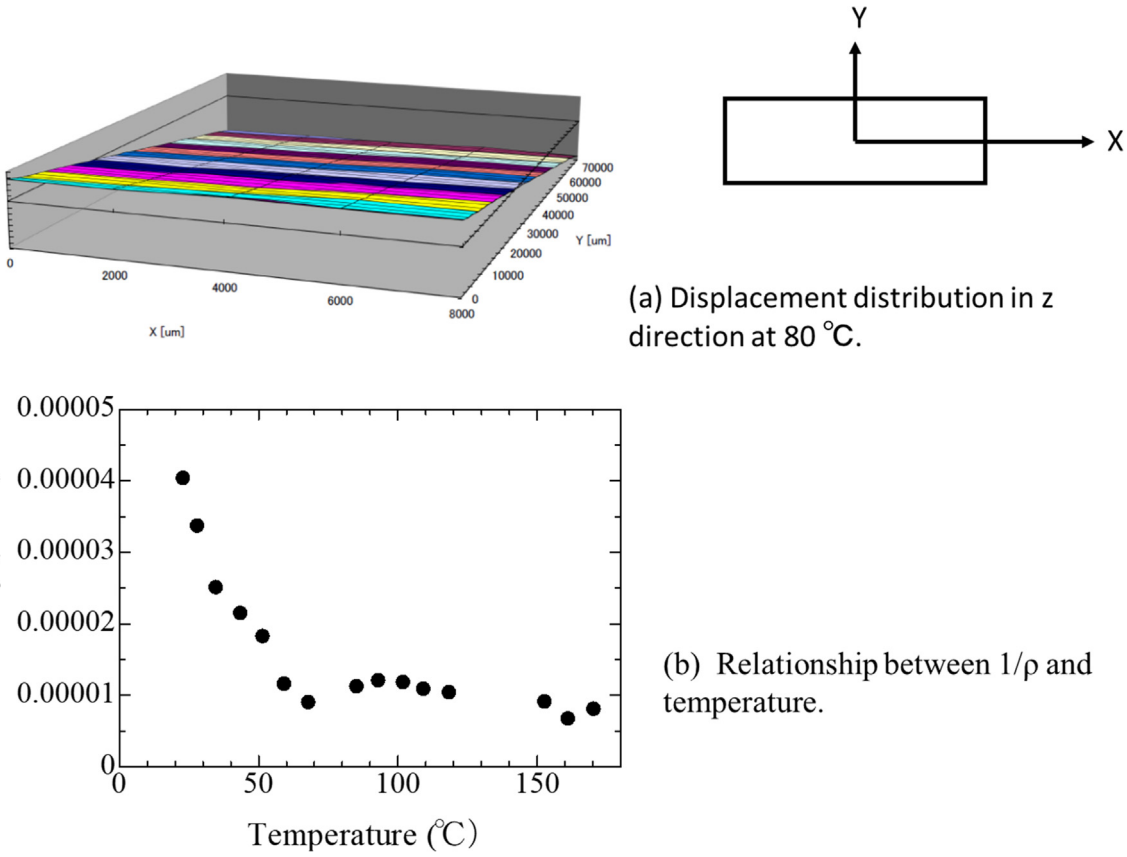

Fig. 6. Relationship between 1/ρ and temperature for the adhesive/aluminum plate specimen.

curvature radius of the specimen, ρ is given in Eq. (3).

$$\frac{1}{\rho} = \frac{(\alpha_1 - \alpha_2)\Delta T}{\frac{z_1 + z_2}{2} + \frac{(E_1 z_1^3 + E_2^3)(E_1 z_1 + E_2 z_2)}{6(z_1 + z_2)E_1 E_2 z_1 z_2}} \quad (3)$$

In this equation, the epoxy adhesive and aluminum adherend are treated as layer 1 and 2, respectively. ΔT is the difference between the stress-free temperature (80 °C) and room temperature (25 °C), z_1 and z_2 are thicknesses of layers 1 and 2, E_1 and E_2 are Young's moduli of layers 1 and 2, and α_1 and α_2 are the coefficients of thermal expansion of layers 1 and 2. In this equation the only unknown value is the apparent thermal expansion coefficient of layer 1. Hence, the thermal expansion coefficient of the adhesive can be obtained by using the material constants of the aluminum plate and elastic moduli in Table 1. Thus, the calculated apparent thermal expansion of the epoxy adhesive was also added in Table 1, wherein the Young's modulus and the coefficient of linear expansion of the adhesive are assumed constant during the temperature change process from the stress-free temperature to the room temperature. Actually, the Young's modulus of the adhesive decreases with increasing the temperature, and the coefficient of linear expansion also depends on the temperature. Therefore, it is different from the linear expansion coefficient of this adhesive at room temperature. The measured value of the linear expansion coefficient of this adhesive at room temperature was 5.95 × 10^{-5}/°C, which is about 1.8 times the apparent coefficient of linear expansion shown in Table 1.

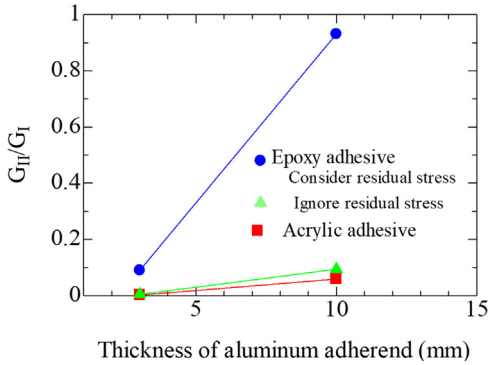

Fig. 7. Effect of aluminum adherend thickness on mode ratio, G_{II}/G_I (Applied load :210 N).

3.2. Results of the FEM analysis

Fig. 7 shows the effect of the aluminum adherend thickness on the

Table 1
Material properties of the adhesives and adherends.

Materials	Moduli of elasticity	Poisson's ratio	Coefficient of thermal expansion
CFRP	Exx = 130.0 GPa, Gxy = 4.0 GPa, Eyy = 9.9 GPa, Gyz = 7.5 GPa, Ezz = 9.9 GPa, Gzx = 4.0 GPa	ν_{xy} = 0.31, ν_{yz} = 0.21, ν_{zx} = 0.0236	2.0 × 10^{-7}/°C (X direction)
Aluminum alloy	E = 71.6 GPa	ν = 0.33	2.36 × 10^{-5}/°C
Epoxy adhesive	E = 3.37 GPa	ν = 0.37	3.23 × 10^{-5}/°C
Acrylic adhesive	E = 0.146 GPa	ν = 0.41	

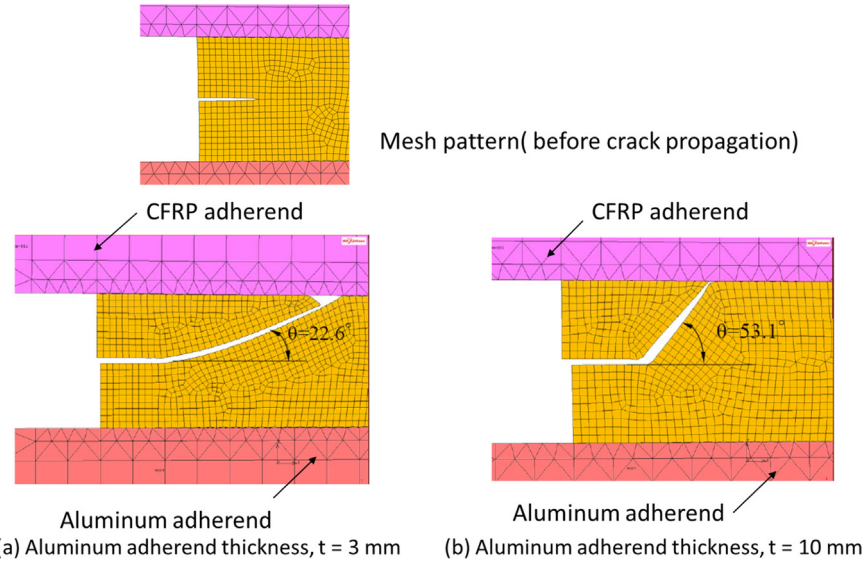

Fig. 8. Effect of aluminum adherend thickness on the crack growth direction, θ, where DCB joints were bonded with the epoxy adhesive (Applied load :210 N).

mode ratio. In Fig. 7, plots of the mode ratio ignoring the effect of residual stress on the epoxy adhesive are also indicated. When the aluminum plate thickness was 3 mm, the G_{II} component was small for both epoxy and acrylic adhesives. However, when the aluminum plate thickness was 10 mm, the G_{II} component was still small for the acrylic adhesive and the epoxy adhesive ignoring the residual stress, whereas that for the epoxy adhesive considering the residual stress is about ten times as large. This means that the restriction for bending deformation due to cooling process from the curing temperature to room temperature of the epoxy adhesive considerably affects the increase in the G_{II} component. This increase in the G_{II} component due to residual stress was also pointed out by Valentin et al. [9].

Fig. 8 shows the effect of aluminum adherend thickness on the crack growth direction for the joints made with epoxy adhesive. The cracks bend to the CFRP side, and crack growth direction, θ increases with increasing aluminum adherend thickness. The crack growth direction, θ is related to the mode ratio as in Fig. 7, that is, θ increases with the increase in G_{II} component. Such a trend has also been observed for another CFRP/aluminum DCB joints [11].

In contrast to the epoxy adhesive, the crack growth direction, θ of the acrylic adhesive was small compared to that of epoxy adhesive as in Fig. 9, which may be due to the lack of residual stress during the curing process. In addition, the flexural rigidity of the CFRP plate was greater than that of the 3 mm aluminum plate and smaller than that of the 10 mm aluminum plate. Hence, the crack growth direction in the joint with the 3 mm aluminum adherend was the reverse of that with 10 mm aluminum. However, similar to the epoxy adhesive, the absolute value of θ increased with increasing aluminum adherend thickness.

4. Experimental results and discussion

Fig. 10 shows the fatigue crack growth rate, da/dN, against the range of total strain energy release rate, $\Delta G_T = G_{Tmax}$-G_{Tmin}, for the DCB specimens with the epoxy and acrylic adhesives. The plots of da/dN against ΔG_T consist of regions I and II. The former region is associated with a fatigue threshold, ΔG_{Tth}, and in the latter region, the Paris relationship is obtained as expressed in Eq. (4).

$$\frac{da}{dN} = k(\Delta G_T)^n \tag{4}$$

In Eq. (4), K and n are crack growth parameters.

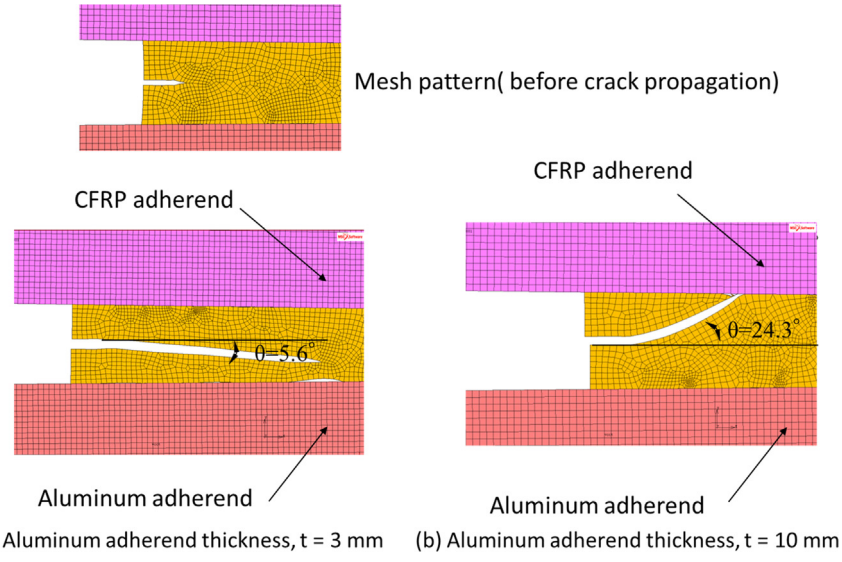

Fig. 9. Effect of aluminum adherend thickness on the crack growth direction, θ, where DCB joints were bonded with the acrylic adhesive (Applied load :210 N).

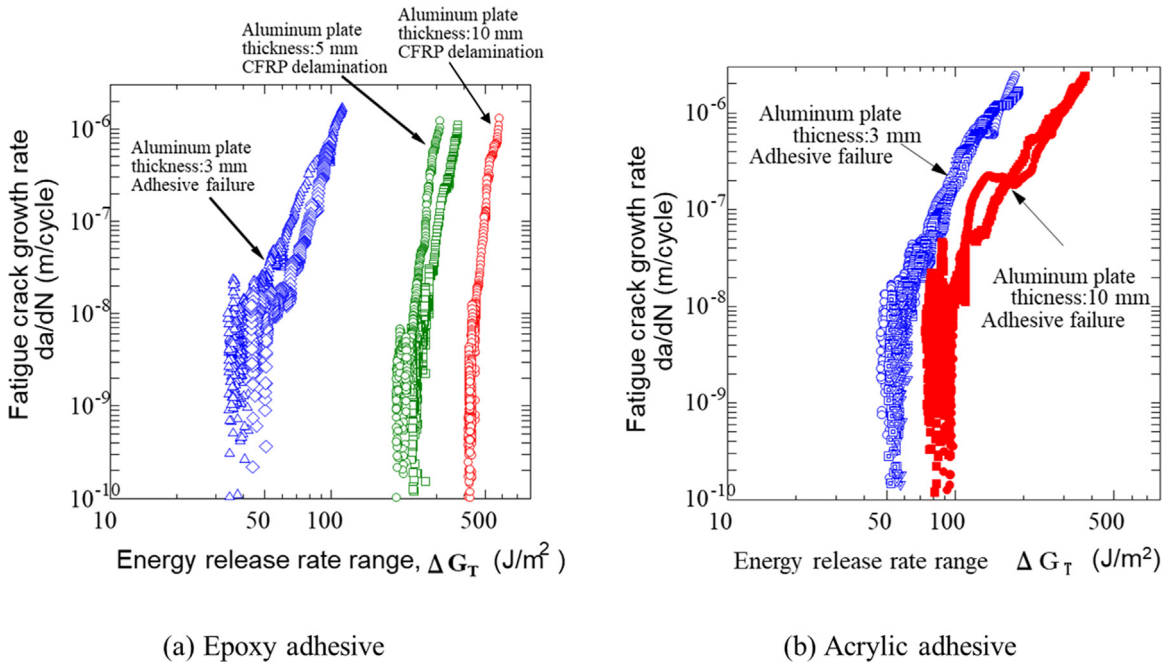

Fig. 10. Fatigue crack propagation curves for the DCB specimens.

For the DCB joints with the epoxy adhesive, as in Fig. 10 (a), cohesive fracture is observed only for the DCB joint with 3 mm aluminum adherend, whereas CFRP delamination is observed for the joints with 5 mm and 10 mm aluminum adherends.

Typical fracture surfaces of the DCB specimens with the epoxy are shown in Fig. 11(a). The fracture surface with the 3 mm aluminum adherend indicates cohesive fracture in the adhesive layer and that with the 10 mm adherend indicates CFRP delamination. This difference in the fracture pattern may be governed by the crack growth direction. As shown in Fig. 8, the simulated crack growth direction, θ increases with increasing aluminum adherend thickness, which means that the fatigue crack tends to propagate in the adhesive layer for a thin aluminum adherend joint, but tends to enter the CFRP plate and probably pass through the matrix and fiber interface for a thick aluminum adherend joint. This simulated trend agrees with fracture pattern mentioned above. Fig. 10 (a) also indicates that ΔG_{th} of the joints with 5 mm and 10 mm adherends are greater than that with 3 mm adherend, wherein the former ΔG_{th} is the threshold of the CFRP delamination, and the latter is the threshold in the adhesive layer. Comparing the 5 and 10 mm aluminum adherend joints, the ΔG_{th} of the joint with 10 mm adherend was greater than that for 5 mm adherend. As in Fig. 7, the G_{II} component increases with increasing aluminum adherend thickness, wherein the increase in G_{II} component usually improves the fracture toughness for many adhesively bonded joints. This trend of ΔG_{th} agrees with that of the calculated mode ratio. Contrary to the trend of ΔG_{th}, the slopes in the Paris region for the joints with 5 mm and 10 mm aluminum adherend thicknesses were steeper than for 3 mm aluminum adherend thickness. The former fracture pattern is delamination and the latter one is cohesive fracture in the adhesive layer. This indicates that a fatigue crack propagates rapidly compared crack propagation in the adhesive layer. A similar trend was also observed for Boron fiber reinforced plastic/aluminum DCB joint [9].

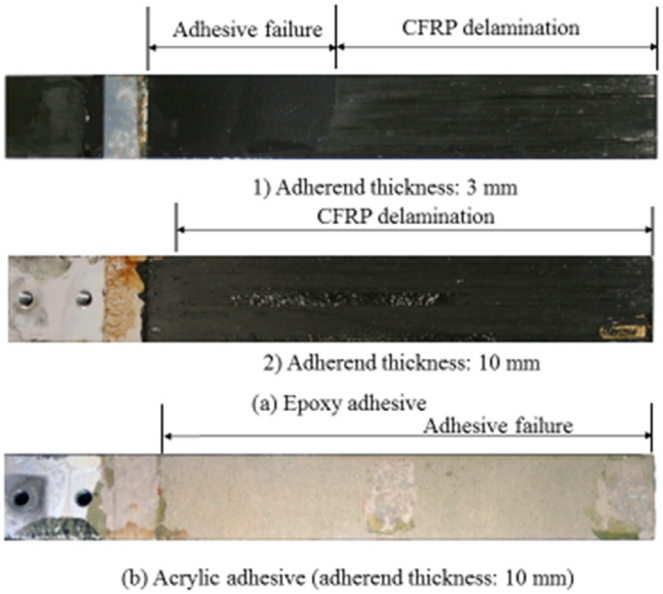

Fig. 11. Macroscopic view of fracture surface of the DCB joints with the epoxy and acrylic adhesives.

For the acrylic adhesive, cohesive fracture was observed irrespective of the aluminum adherend thickness, as shown in Fig. 10 (b). A typical fracture surface of the DCB specimens with the acrylic adhesive is shown in Fig. 11(b). As mentioned above, the fracture pattern is governed by the crack growth direction. As in Fig. 9, the simulated crack growth direction, θ for the DCB joint with acrylic adhesive also increases with increasing aluminum adherend thickness. However the crack growth direction, θ with the acrylic adhesive was smaller than that with the epoxy adhesive, especially for the DCB joints with 10-mm aluminum adherend thickness, while θ with the acrylic adhesive was less than half that of the epoxy adhesive. However, the crack reaches the CFRP interface after only a few mm crack growth. After the cracks arrive at the interface, the crack with the epoxy adhesive propagate in the CFRP layer and the crack with the acrylic adhesive propagates in the adhesive layer. Such a difference in the crack propagation path may be due to the difference in strength between the interface and the adhesive.

This figure shows that ΔG_{th} increases with increasing aluminum adherend thickness, similar to the epoxy adhesive, although the increase of ΔG_{th} is smaller. This may be related to the following tendency: similarly to DCB joints with epoxy adhesive, the G_{II} component for the

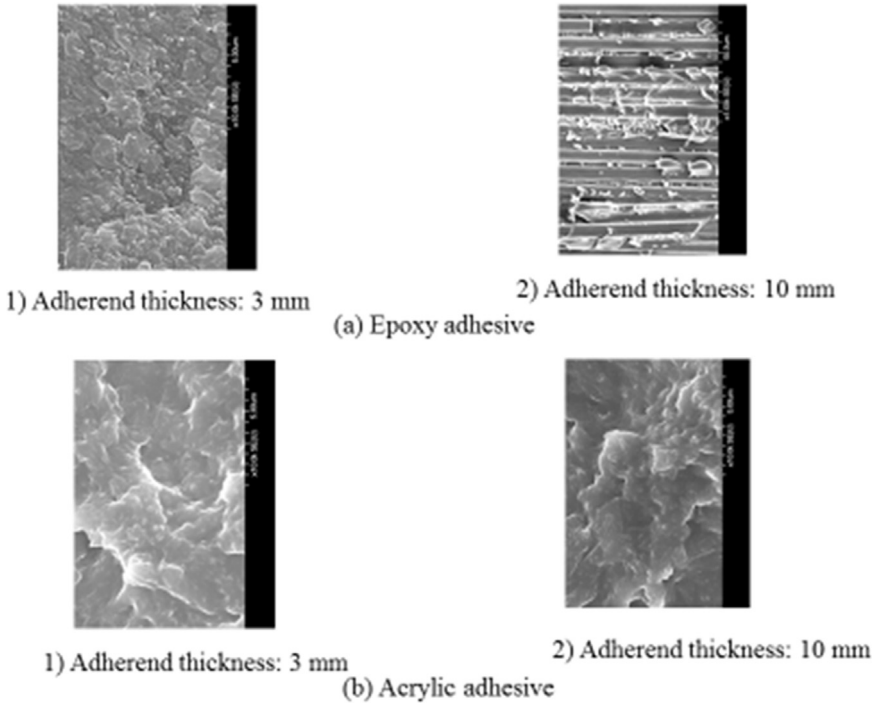

Fig. 12. SEM observation of the fracture surfaces.

acrylic adhesive increased with increasing aluminum adherend thickness as in Fig. 7. However the increase in G_{II} component was small compared to the epoxy adhesive. In contrast, the slopes in the Paris region for the joint with 5 mm adherend thickness was nearly equal to that with 10 mm aluminum adherend thicknesses. When comparing the slopes of the acrylic and epoxy adhesive with cohesive fracture, the slope with the epoxy adhesive is a little steeper than that with the acrylic adhesive.

Fig. 12 shows SEM images of fracture surfaces of the epoxy and acrylic adhesives. For the epoxy adhesive, two types of fracture pattern are indicated in Fig. 12(a), depending on the aluminum adherend thickness. One is cohesive fracture in the adhesive layer, which was observed in the surface with the 3 mm aluminum adherend, and the other is delamination of the CFRP which was observed in the surface with the 10 mm aluminum adherend. The cohesive fracture surface with the epoxy adhesive suggests an aggregation of small clusters, and the deformation of the fracture surface is small. In the delaminated surface, carbon fibers are exposed, and the matrix resin is also observed. In contrast, cohesive fracture is observed for the fracture surfaces with the acrylic adhesive irrespective of the aluminum adherend thickness, as in Fig. 12(b). Compared to the cohesive fracture surface with the epoxy adhesive, large deformation was observed for the acrylic adhesive, and the morphology of the fracture surface did not depend on the aluminum adherend thickness. Furthermore, SEM images for the adhesive fracture surfaces shows the presence of shear cusps which suggests a mode **II** -driven failure.

5. Conclusions

Fatigue tests were conducted on the adhesively bonded CFRP/aluminum double cantilever beam (DCB) joints with acrylic and epoxy adhesives, and the fatigue crack growth rate of the acrylic adhesive was compared with that of the epoxy adhesive. The main results obtained were as follows:

1. The effects of the thickness ratios of the adherend on the mode ratio and crack propagation path were investigated by finite element analysis. The G_{II} component with 3 mm aluminum adherend thickness was small for both epoxy and acrylic adhesives. However, the G_{II} components with 10 mm aluminum adherend thickness was still small for the acrylic adhesive, while that with the epoxy adhesive was about 10 times as large. The crack growth direction, θ increased with increasing aluminum adherend thickness for the both the epoxy and acrylic adhesives, but the increase in crack growth direction, θ for the acrylic adhesive was small compared to that with epoxy adhesive.
2. For the epoxy adhesive, cohesive fracture was observed only for DCB joint with 3 mm aluminum adherend thickness, and CFRP delamination was observed for the joints with 5 mm and 10 mm aluminum adherend thicknesses. For the acrylic adhesive, cohesive fracture was observed irrespective of the aluminum adherend thickness.
3. For the epoxy adhesive, ΔG_{th} of the joints with 5 mm and 10 mm adherend thicknesses were greater than that with 3 mm adherend thickness. The former ΔG_{th} is the threshold of the CFRP delamination, while the latter one is the threshold in the adhesive layer. Contrary to the trend of ΔG_{th}, the slopes in the Paris region for the joints with 5 mm and 10 mm aluminum adherend thicknesses were steeper than that with 3 mm aluminum adherend thickness.
4. For the acrylic adhesive, ΔG_{th} with the acrylic adhesive increased with increasing aluminum adherend thickness. The slopes in the Paris region for the joint with 5 mm was nearly equal to that with 10 mm aluminum adherend thicknesses. Comparing the slope with the acrylic adhesive that of epoxy adhesive with 3 mm aluminum adherend thickness, the slope with the epoxy adhesive was a little steeper.

References

[1] Abdel Wahab MM, Ashroft IA, Crocombe AD, Smith PA. Finite element prediction life time in composite bonded joints. Compos: Part A 2004;35:213–22.
[2] Erpolat S, Ashcroft IA, Crocombe AD, Wahab MA. On the analytical determination of strain energy release rate in bonded DCB joints. Eng Frac Mech 2004;71:1393–401.
[3] Casas-Rodriguez JP, Ashcroft IA. Silberschmidt. Dalamination in adhesively bonded CFRP joints: standard fatigue, impact-fatigue and intermittent impact. Comp Sci Technol 2008;68:2401–9.
[4] Meneghtti G, Quaresimin M, Ricotta M. Influence of the interface ply orientation on

the fatigue behavior of bonded joints in composite materials. Int J Fatigue 2010;32:82–93.
[5] Fernandez MV, MFSF de Moura, da Silva, Marques LFM, Composite AT. bonded joints under mode I fatigue loading. Int J Adhes Adhes 2011;31:280–5.
[6] Meneghtti G, Quaresimin M, Ricotta M. Damage mechanisms in composite bonded joints under fatigue loading. Compos: Part B 2012;43:210–20.
[7] Bernasconi A, Jamil A, Moroni F, Pirondi A. A study on fatigue propagation in thick composite adhesively bonded joints. Int J Fatigue 2013;50:18–25.
[8] Fernandez MV, de Moura MFSF, da Silva LFM, Marques AT. Mixed-mode I + II fatigue/fracture characterization of composite bonded joints using the Sinle-Leg Bending test. Compos: Part A 2013:63–9.
[9] Valentin RV, Butkus LM, Johnson WS. A finite element and experimental evaluation of boron-epoxy doublers bonded to an aluminum substrate. J Comp Technol Res 1998;20:108–19.
[10] Cheuk PT, Tong L, Wang CH, Baker A, Chalkley P. Fatigue crack growth in adhesively bonded composite-metal double-lap joints. Comp Struct 2002;57:109–15.
[11] Ishii K, Imanaka M, Nakayama H. Fatigue crack propagation behavior of adhesively-bonded CFRP/aluminum joints. J Adhes Sci Technol 2007;21:153–67.
[12] Hedayati R, Khouzani SG, Jahanbaksshi M. Investigation of debonding propagation in aluminum/composite joints under fatigue loading. J Adhes Sci Technol 2015;29:59–73.
[13] de Freitas ST, Sinke J. Failure analysis of adhesively-bonded metal-skin-to-composite-stiffener: effect of temperature and cyclic loading. Comp Struct 2017;166:27–37.
[14] Lefebvre DR, Dillard AD. A stress singularity approach for the prediction of fatigue crack initiation. Part 1:Theory J Adhes 1999;70:119–38.
[15] Ashcroft IA, Crocombe AD. Modeling fatigue in adhesively bonded joints. In: da Silva LFM, Ochsner A, editors. Modelig of adhesively bonded joints. Springer; 2008.
[16] Graner Solana A, Crocombe AD, Ashcroft IA. Fatigue life and backface strain preictions in adhesively bonded joints. Int J Adhes Adhes 2010;30:36–42.
[17] Hafiz TA, Abdel-Wahab MM, Crocombe AD, Smith PA. Mixed-mode fatigue growrh in FM73 bonded joints. Int J Adhes Adhes 2013;40:188–96.
[18] Pereira AB, de Morais AB. Strength of adhesively bonded stainless steel joints. Int J Adhes Adhes 2003;23:315–22.
[19] Boyd SW, Winkle IE, Day AH. Bonded butt joints in pultruded GRP panels-an experimental study. Int J Adhes Adhes 2004;24:263–75.
[20] de Castro J, Keller T. Ductile double-lap joints form brittle GFRP laminates and ductile adhesives, Part 1:experimental investigation. Compos Part B 2008;39:271–81.
[21] Gallio G, Lombardi M, Rovarino D, Fino P. Montanaro, Influence of the mechanical behavior of different adhesives on an interference-fit cylindrical joint. Int J Adhes Adhes 2013;47:63–8.
[22] Yadollahi M, Barkhordari S, Gholamali I, Farhoudian S. Effect of nanofillers on adhesion strength of steel joints bonded with acrylic adhesive. Sci Tech Weld Join 2015;20:443–50.
[23] Imanaka M, Liu X, Kimoto M. Comparison of fracture behavior between acrylic and epoxy adhesives. Int J Adhes Adhes 2017;75:31–9.
[24] Kim H-B, Naito K, Oguma H. Fatigue crack growth properties of a two-part acrylic-based adhesive in an adhesive bonded joint: double cantilever-beam tests under Mode I loading. Int J Fatigue 2017;98:286–95.
[25] Hutchinson JW, Suo Z. Mixed mode cracking in layered materials. In: Hutchinson JW, Wu TW, editors. Advances in applied mechanics, 29. Elsevier; 1991. p. 63191.